optica

High-harmonic generation at 250 MHz with photon energies exceeding 100 eV

H. CARSTENS,[1,2] M. HÖGNER,[1,2] T. SAULE,[1,2] S. HOLZBERGER,[1,2] N. LILIENFEIN,[1,2] A. GUGGENMOS,[1,2] C. JOCHER,[3] T. EIDAM,[3] D. ESSER,[5] V. TOSA,[6] V. PERVAK,[2] J. LIMPERT,[3,4] A. TÜNNERMANN,[3,4] U. KLEINEBERG,[1,2] F. KRAUSZ,[1,2] AND I. PUPEZA[1,2,*]

[1]*Max-Planck-Institut für Quantenoptik, Hans-Kopfermann-Str. 1, 85748 Garching, Germany*
[2]*Ludwig-Maximilians-Universität München, Am Coulombwall 1, 85748 Garching, Germany*
[3]*Friedrich-Schiller-Universität Jena, Institut für Angewandte Physik, Albert-Einstein-Straße 15, 07745 Jena, Germany*
[4]*Fraunhofer Institut für Angewandte Optik und Feinmechanik, Albert-Einstein-Straße 7, 07745 Jena, Germany*
[5]*Fraunhofer-Institut für Lasertechnik, Steinbachstraße 15, 52074 Aachen, Germany*
[6]*National Institute for R&D Isotopic and Molecular Technologies, Donath 69-103, 400293 Cluj Napoca, Romania*
**Corresponding author: ioachim.pupeza@mpq.mpg.de*

Received 23 December 2015; revised 23 February 2016; accepted 24 February 2016 (Doc. ID 256128); published 29 March 2016

Ultrafast spectroscopy in the extreme ultraviolet demands for ever-higher pulse repetition rates and photon energies. Here, we drive cavity-enhanced high-order harmonic generation (HHG) at a repetition rate of 250 MHz, with 30 fs pulses and an average power of 10 kW. Employing an optimized cavity geometry and a high-pressure gas target, we couple out nano-watt-level harmonics at photon energies around 100 eV. This constitutes an improvement of more than two orders of magnitude over previous megahertz-repetition-rate HHG experiments and paves the way toward high-photon-energy frequency-comb spectroscopy and toward pump-probe photoelectron microscopy and spectroscopy at unprecedented repetition rates.

OCIS codes: (190.2620) Harmonic generation and mixing; (320.0320) Ultrafast optics.

http://dx.doi.org/10.1364/OPTICA.3.000366

Coherent, extreme ultraviolet (XUV) radiation obtained via the high-order harmonic generation (HHG) of visible or near-infrared lasers has enabled manifold applications in atomic, molecular, and solid-state physics [1]. While for applications like nonlinear physics in the XUV spectral range, a large number of XUV photons per pulse is the most critical requirement, there has also been a strong interest in systems operating with repetition rates in the range of several tens of megahertz. For instance, frequency comb spectroscopy benefits from a high repetition rate since the power per comb line is proportional to the repetition rate. Furthermore, a high repetition rate facilitates data analysis in most cases, e.g., if multiple resonances are simultaneously excited [2]. It has been shown that HHG preserves the coherence of the driving frequency comb [3] and direct XUV frequency comb spectroscopy has been demonstrated with photon energies of about 20 eV [4]. The extension of such sources to higher photon energies would enable numerous applications and insights into fundamental physics. For example, quantum electrodynamic corrections for the electronic energy levels of atoms scale with Z^4 [5], which motivates the spectroscopy of hydrogen-like ions, such as He^+ ($Z = 2$) or Li^{2+} ($Z = 3$). The two-photon 1s-2s transition for He^+ is at 40 eV (e.g., 20 eV + 20 eV or 39 eV + 1 eV) and for Li^{2+} at 91 eV (e.g., 45.5 eV + 45.5 eV or 90 eV + 1 eV). There is also a low-lying nuclear transition of ^{235}U at 76 eV [6], which could serve as a reference for future nuclear clocks.

HHG requires intensities on the order of $10^{14}\ \mathrm{W/cm^2}$, which usually limits the repetition rate of the driving source to less than 1 MHz. Only very recently has a high photon flux at energies up to 35 eV been demonstrated in a single-pass HHG experiment driven by a 10 MHz high-power laser system delivering 30 fs pulses with 70 W of average power [7]. In order to further increase the repetition rate and/or the average power available for HHG, the pulses of a high-repetition-rate front end can be coherently stacked in a passive optical resonator, a so-called enhancement cavity (EC) [8]. In ECs employing purely reflective elements, average powers on the megawatt-scale have been achieved with ultrashort pulses [9]. To efficiently drive HHG, however, pulses as short as possible are desirable. The shortest pulse duration employed so far for kilowatt-level average-power cavity-enhanced HHG was 60 fs [10]. By coupling out the XUV radiation through a tiny hole on the optical axis, which is drilled into a cavity mirror, photon energies exceeding 100 eV have been demonstrated at 80 MHz [10]. Together with the prospect of enhancing phase-stable few-cycle pulses [11,12], these considerations justify efforts toward driving intracavity HHG with ever-shorter pulses at multi-kilowatt average-power levels.

In this work, we explore the potential and the limitations of decreasing the pulse duration and increasing the repetition rate in cavity-enhanced HHG by driving the nonlinear conversion with 10 kW, 30 fs pulses at a repetition rate of 250 MHz. The experimental setup is depicted in Fig. 1. It is based on the system

Corrected 30 March 2016

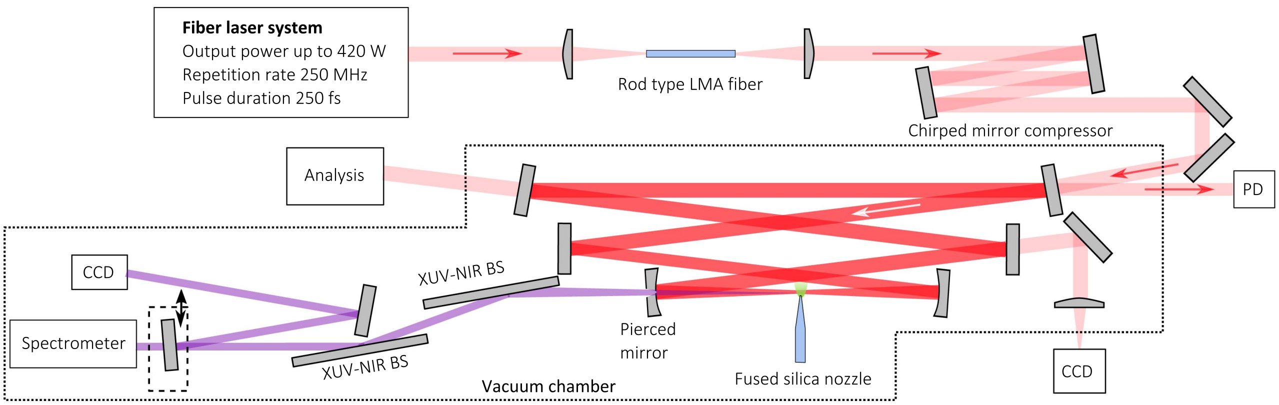

Fig. 1. Schematic of the experimental setup. After compression, the pulses are coupled into the EC. The cavity beam on the pierced mirror is imaged onto a CCD. The intracavity power is measured via the calibrated transmission of one cavity mirror with a thermal power detector with a flat response over the entire spectrum. PD, photodiode.

described in detail in [9]. An ytterbium-fiber chirped-pulse amplification system delivering 250 fs pulses at a repetition rate of 250 MHz is used as the driving laser [13]. The pulses are spectrally broadened in a rod-type fiber (mode field diameter 59 μm) and subsequently compressed to 30 fs using chirped mirrors at an average output power of 170 W. The resulting bandwidth of about 120 nm is chosen such that the pulses can be enhanced with broadband quarter-wave-stack-like mirrors consisting of alternating layers of Nb_2O_5 and SiO_2 with a flat phase and uniform reflectivity [12]. Note that for fiber amplifiers, the pulse energy is limited by nonlinear effects, while very high average powers are attainable. In our experiment, despite the high repetition rate, the pulse energy is higher than in [4,10].

For our first experiment, which is aimed at power scaling with 30 fs pulses, we set up a bow-tie cavity consisting of six mirrors without an XUV output coupler. Except for the input coupler, which was coated on a fused-silica substrate, all of the mirrors used Corning ULE substrates [9]. The focusing mirrors have a radius of curvature of 600 mm and the cavity length is 4800 mm, such that four pulses circulate in the EC. The cavity is operated close to the inner stability edge, which ensures large spot sizes on all the mirrors. This configuration is robust against misalignment [14] and thermal effects [9]. Using the method described in [9], we estimate the absorption of the broadband mirrors to exceed that of Ta_2O_5–SiO_2 quarter-wave stacks by a factor of 5. Furthermore, the damage fluence is expected to be significantly lower due to the smaller bandgap of Nb_2O_5 and due to the shorter pulse duration [15]. The maximum intracavity average power achieved in this cavity with 30 fs pulses was 20 kW.

For output coupling the generated XUV radiation, a pierced mirror [10] is employed. So far, this has been the only output coupling method demonstrated for photon energies exceeding 40 eV. It is intrinsically dispersion free and polarization insensitive. Mirrors with holes drilled using the same technique as in [10,16] and with the broadband coating described above were repeatedly damaged at relatively low powers of only a few kilowatts, irrespective of the substrate material (ULE or fused silica). In addition, the pierced mirrors with ULE substrates heated up significantly, leading to the misalignment of the cavity due to mirror mount deformations. Reliable operation at the 10 kW power level was enabled by using pierced mirrors with improved-quality hole edges. In contrast to [10,16], the holes were drilled in a conventional geometry and with shorter pulses and less pulse energy. After the breakthrough of the drilling, the holes' edges were drilled again, resulting in sharper edges. In the final step, the substrates were tempered to reduce bulging and relieve stress at the edges [16]. These mirrors were available with fused-silica substrates only, which resulted in a considerable thermal lens in the EC. Due to the front-side drilling, the clear aperture of the opening determining the XUV output coupling efficiency is about 25% smaller than the outer diameter, which determines the losses for the fundamental light. A further performance improvement is expected with ULE substrates, which mitigate thermal lensing.

For the generation of high photon energies in the 100 eV range in neon, intensities exceeding 10^{14} W/cm^2 are required. To reach these intensities at a 250 MHz repetition rate, even with 30 fs pulses and 10 kW of average power, tight focusing with a focus radius of less than 15 μm is necessary. In principle, phase matching can be achieved by compensating for the Gouy phase shift with the dispersion of the gas target even in such a tight focusing geometry [17]. However, due to the strong Gouy shift and the weak dispersion of neon, high gas pressures are required. We estimate the phase-matching pressure to be about 5 bar in the target [17,18] for our geometry. To reach these pressures, the nozzles must be placed very close to the laser focus and high backing pressures must be applied behind the nozzle. We employed endfire nozzles with an opening diameter of 100 μm made of fused silica to avoid melting during the experiment. In order to keep the ambient pressure in the chamber below 10^{-2} mbar at backing pressures of up to 12 bar of neon, a 1600 l/s turbo pump with a 110-m^3/h pre-pump was used.

A common challenge to all high-average-power HHG experiments is the separation of the driving laser field from the generated harmonic radiation. Here, a significant portion of near-infrared (NIR) light leaks through the pierced mirror [10]. If the losses introduced by the hole (0.5%) dominate the total losses and for an impedance-matched case, i.e., when the losses are equal to the input coupler transmission, half of the input coupled power exits the resonator through the hole, while the other half is scattered at the hole. In our case, the power transmitted through the hole is on the order of 50 W, a power level that is far too high for thin metallic filters typically used for NIR suppression. For the separation of the XUV and NIR radiation, grazing-incidence plates (angle of incidence >70°) with an anti-reflection (AR) coating for the NIR with SiO_2 or HfO_2 as the top layer were used in [10,19,20]. These coatings suffer from a low reflectivity of about 20% for a photon energy around 100 eV. Here, we use an alternative design with Nb_2O_5 as the top layer. Figure 2 shows the calculated reflectivity in the XUV of such beam splitters [21]. An AR coating for the NIR can be designed for either s- or p-polarization. Examples are shown in the lower panel of Fig. 2 for a bandwidth corresponding to the 30 fs pulses. For s-polarization, the reflection of the AR coating is slightly higher, but the reflectivity in the XUV, in particular for photon energies lower than 75 eV, is also higher (see Fig. 2). In the experiments, the design for p-polarization is used, which has a 135 nm thick Nb_2O_5 layer on top, resulting in a reflectivity of 75% at 100 eV. This allows for a strong attenuation of the NIR light, so that thin metal filters can be subsequently used in the beam.

In order to obtain high photon energies, the pulses were focused with 200 mm radius-of-curvature spherical mirrors to a spot size of $10 \times 18\ \mu m^2$, resulting in a peak intensity of about $3 \times 10^{14}\ W/cm^2$ in a neon target. The generated XUV radiation was analyzed with an imaging spectrometer equipped with a CCD. A spectrum is shown in Fig. 3. The power spectral density of the spectra refers to the output coupled power directly behind the curved mirror. The power measurement was done by filtering a single harmonic order with narrow-band mirrors at 13.2 nm and then detecting it with an XUV-CCD. We measured 1.3 nW in the 79th harmonic order at 94 eV, which corresponds to 9×10^7 photons/s in a 2% bandwidth. The cutoff is located at about 110 eV. However, in this range, the quantum efficiency of the CCD drops abruptly, i.e., higher photon energies might not have been detected. The intensity is in good agreement with the intensity clamping level predicted by the model developed in [11] for 5 bar of pressure in a 200-μm-long gas target.

The beam profile of the 79th harmonic is shown in Fig. 3. In order to estimate the output coupling efficiency, we conducted simulations of the generation and propagation of the harmonic radiation for our experimental conditions with the numerical models described in [22,23]. These simulations reveal a divergence that is significantly higher than that predicted by the simplified model used in [10], which is due to the dipole phase. The divergence strongly depends on the harmonic order and the position of the gas jet relative to the focus. For H79, an optimum of the output coupled power is predicted for 5 bar of neon and a nozzle placed half a Rayleigh length before the focus. This pressure in the target agrees with the gas flow simulations for our gas nozzle and 11 bar of backing pressure. The output coupling efficiency through the aperture with a diameter of 120 μm in this case is about 5%. The losses introduced to the fundamental light by the opening in the mirror with an outer diameter of 180 μm are about 0.4%. Increasing the inner aperture to 180 μm as well would almost double the output coupling efficiency. Improved pierced mirrors, preferably in ULE substrates, are therefore highly desirable. The spatial intensity structure of the beam profile (see Fig. 3) is owed to diffraction at the pierced mirror, as can be seen from the simulation in Fig. 3. For the simulation, the shape of the opening was used, as determined from a microscope picture, and a spherical wave impinging on the hole was assumed. The propagation of the clipped beam with the Fresnel formula according to the experimental geometry gives good agreement for the beam size and structure. Even though the beam exhibits a strong diffraction pattern, it could still be focused to a smooth beam profile, as can be seen from the simulation.

With argon and xenon, the measured power levels (2.5 μW at 30 nm) were similar to those reported in [10], although all parameters, in particular the shorter driving pulses, higher peak intensity, and higher NIR power, are expected to improve the photon flux. We attribute this observation to cumulative effects [24–26] due to the high repetition rate of 250 MHz. Here, the time between two successive pulses is only 4 ns. During this time, only a few percent of the xenon atoms leave the interaction region. To increase the particle speed, we mixed the gas flow of xenon with helium [26], which improved the XUV photon flux by 30% (3.6 μW at 61 nm) compared to a pure xenon gas target, and

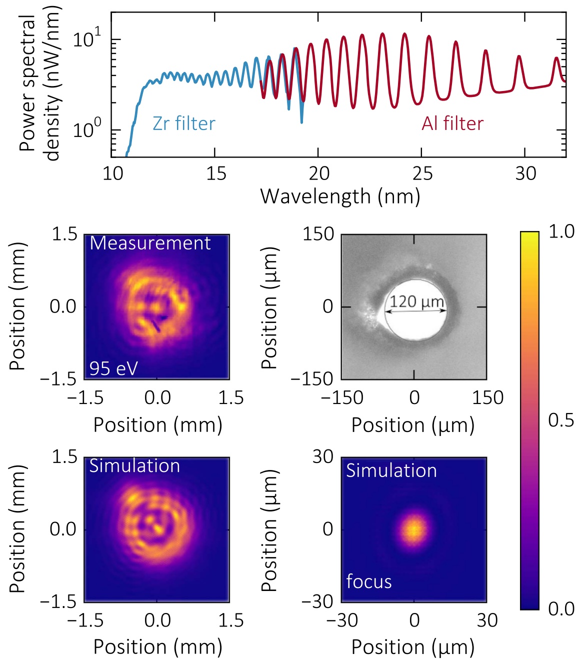

Fig. 3. (Upper panel) Calibrated HHG spectrum from neon using zirconium or aluminum filters. (Lower panel) The measured beam profile of H79 at 94 eV and the corresponding simulation, the simulated focus beam profile with a focal length of 50 mm, and a picture of the pierced mirror inner aperture. The distance between the pierced mirror and detector was 1.4 m.

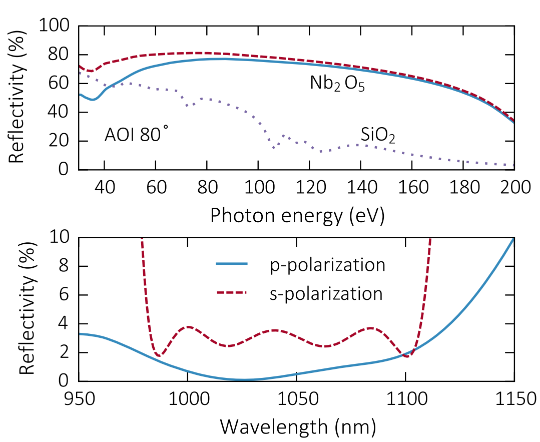

Fig. 2. Calculated reflectivity of the XUV-NIR beam splitter in the XUV (upper panel) and NIR (lower panel). Nb_2O_5 exhibits a good reflectivity even for the 100 eV level.

confirmed that the photon flux in this high-repetition-rate regime is limited by cumulative effects. Mixing helium (mass: 4 u) with the gas in which the harmonic radiation is generated helps most for heavy gases such as xenon (mass: 131 u). We did not try this with neon, as it is intrinsically fast (mass: 20 u), and because the mixture of helium and neon with an optimized pressure would have exceeded the capacity of our turbo pump. As these effects are a general limitation for high-repetition-rate HHG, future investigations should address the mechanisms of the plasma recombination and its effect on high-harmonic generation. One could, for example, employ a pulse picker to measure the HHG conversion efficiency for a variable repetition rate while keeping the parameters of the single pulses constant. In [7], this was already done for a repetition rate of up to 10 MHz: while the conversion efficiency stayed constant for an increase of the repetition rate from 234 kHz to 4 MHz, it decreased by 30% for an increase from 4 to 10 MHz. With an enhancement cavity, this experiment is possible at higher repetition rates and, in addition, ionization dynamics could be measured [27].

In conclusion, we have investigated intracavity HHG at a repetition rate of 250 MHz, driven by 30 fs pulses with multi-kilowatt average powers. The output coupled photon flux around 100 eV was improved by more than two orders of magnitude over previous work at an 80 MHz repetition rate. Together with a stabilized offset frequency, this would correspond to more than 500 times more power per comb line for frequency comb spectroscopy in this spectral range. This is enabled by several factors: first, the short pulses of 30-fs allow for a higher intensity [11] compared to previous results [10], and thus a higher dipole moment and higher cutoff. Also, phase matching was achieved with an improved experimental apparatus, allowing for a high density gas target. In addition, the fundamental power was three times higher than in [10]. The generated photon flux in our experiment is comparable to record values at a sub-megahertz repetition rate [17]. However, output coupling limits the XUV flux usable outside of the cavity to less than 10% of the generated photons. Apart from improved pierced mirrors, a higher output coupling efficiency can be reached, for example, by quasi-imaging [23] or with Bessel–Gauss beams [28]. Advancing the demonstrated system toward bandwidths sufficiently broad to allow the enhancement of few-cycle pulses with a controlled carrier-envelope phase [12] will pave the way toward the generation of isolated attosecond pulses from enhancement cavities at multi-megahertz repetition rates.

Funding. Fraunhofer-Max-Planck (MEGAS); European Research Council (ERC) (617173); Deutsche Forschungsgemeinschaft (DFG) (MAP); Unitatea Executiva pentru Finantarea Invatamantului Superior, a Cercetarii, Dezvoltarii si Inovarii (UEFISCDI) (PN-II-ID-PCE-2012-4-0342).

REFERENCES

1. F. Krausz, Rev. Mod. Phys. **81**, 163 (2009).
2. M. Herrmann, M. Haas, U. D. Jentschura, F. Kottmann, D. Leibfried, G. Saathoff, C. Gohle, A. Ozawa, V. Batteiger, S. Knünz, N. Kolachevsky, H. A. Schüssler, T. W. Hänsch, and T. Udem, Phys. Rev. A **79**, 052505 (2009).
3. C. Benko, T. K. Allison, A. Cingöz, L. Hua, F. Labaye, D. C. Yost, and J. Ye, Nat. Photonics **8**, 530 (2014).
4. A. Cingöz, D. C. Yost, T. K. Allison, A. Ruehl, M. E. Fermann, I. Hartl, and J. Ye, Nature **482**, 68 (2012).
5. Z.-C. Yan, W. Nörtershäuser, and G. W. F. Drake, Phys. Rev. Lett. **100**, 243002 (2008).
6. A. D. Panov, J. Exp. Theor. Phys. **85**, 313 (1997).
7. S. Hädrich, M. Krebs, A. Hoffmann, A. Klenke, J. Rothhardt, J. Limpert, and A. Tünnermann, Light: Sci. Appl. **4**, e320 (2015).
8. C. Gohle, T. Udem, M. Herrmann, J. Rauschenberger, R. Holzwarth, H. A. Schuessler, F. Krausz, and T. W. Hänsch, Nature **436**, 234 (2005).
9. H. Carstens, N. Lilienfein, S. Holzberger, C. Jocher, T. Eidam, J. Limpert, A. Tünnermann, J. Weitenberg, D. C. Yost, A. Alghamdi, Z. Alahmed, A. Azzeer, A. Apolonski, E. Fill, F. Krausz, and I. Pupeza, Opt. Lett. **39**, 2595 (2014).
10. I. Pupeza, S. Holzberger, T. Eidam, H. Carstens, D. Esser, J. Weitenberg, P. Rußbüldt, J. Rauschenberger, J. Limpert, T. Udem, A. Tünnermann, T. W. Hänsch, A. Apolonski, F. Krausz, and E. Fill, Nat. Photonics **7**, 608 (2013).
11. S. Holzberger, N. Lilienfein, H. Carstens, T. Saule, M. Högner, F. Lücking, M. Trubetskov, V. Pervak, T. Eidam, J. Limpert, A. Tünnermann, E. Fill, F. Krausz, and I. Pupeza, Phys. Rev. Lett. **115**, 023902 (2015).
12. S. Holzberger, N. Lilienfein, M. Trubetskov, H. Carstens, F. Lücking, V. Pervak, F. Krausz, and I. Pupeza, Opt. Lett. **40**, 2165 (2015).
13. C. Jocher, T. Eidam, S. Hädrich, J. Limpert, and A. Tünnermann, Opt. Lett. **37**, 4407 (2012).
14. H. Carstens, S. Holzberger, J. Kaster, J. Weitenberg, V. Pervak, A. Apolonski, E. Fill, F. Krausz, and I. Pupeza, Opt. Express **21**, 11606 (2013).
15. M. Mero, J. Liu, W. Rudolph, D. Ristau, and K. Starke, Phys. Rev. B **71**, 115109 (2005).
16. D. Esser, J. Weitenberg, W. Bröring, I. Pupeza, S. Holzberger, and H.-D. Hoffmann, Opt. Express **21**, 26797 (2013).
17. J. Rothhardt, S. Hädrich, A. Klenke, S. Demmler, A. Hoffmann, T. Gotschall, T. Eidam, M. Krebs, J. Limpert, and A. Tünnermann, Opt. Lett. **39**, 5224 (2014).
18. C. M. Heyl, J. Güdde, A. L'Huillier, and U. Höfer, J. Phys. B **45**, 74020 (2012).
19. O. Pronin, J. Brons, C. Grasse, V. Pervak, G. Boehm, M.-C. Amann, V. L. Kalashnikov, A. Apolonski, and F. Krausz, Opt. Lett. **36**, 4746 (2011).
20. S. Hädrich, A. Klenke, J. Rothhardt, M. Krebs, A. Hoffmann, O. Pronin, V. Pervak, J. Limpert, and A. Tünnermann, Nat. Photonics **8**, 779 (2014).
21. B. L. Henke, E. M. Gullikson, and J. C. Davis, At. Data Nucl. Data Tables **54**, 181 (1993).
22. E. Takahashi, V. Tosa, Y. Nabekawa, and K. Midorikawa, Phys. Rev. A **68**, 023808 (2003).
23. I. Pupeza, M. Högner, J. Weitenberg, S. Holzberger, D. Esser, T. Eidam, J. Limpert, A. Tünnermann, E. Fill, and V. S. Yakovlev, Phys. Rev. Lett. **112**, 103902 (2014).
24. T. K. Allison, A. Cingöz, D. C. Yost, and J. Ye, Phys. Rev. Lett. **107**, 183903 (2011).
25. D. R. Carlson, J. Lee, J. Mongelli, E. M. Wright, and R. J. Jones, Opt. Lett. **36**, 2991 (2011).
26. A. K. Mills, T. J. Hammond, M. H. C. Lam, and D. J. Jones, J. Phys. B **45**, 142001 (2012).
27. D. R. Carlson, T. H. Wu, and R. J. Jones, in *2015 European Conference on Lasers and Electro-Optics–European Quantum Electronics Conference* (Optical Society of America, 2015), paper CF_9_5.
28. W. P. Putnam, D. N. Schimpf, G. Abram, and F. X. Kärtner, Opt. Express **20**, 24429 (2012).